Reducing Emissions by Optimising the Fuel Injector Match with the Combustion Chamber Geometry for a Marine Medium-Speed Diesel Engine

Nao Hu[1, 2,*], Peilin Zhou[1], Jianguo Yang[2, 3]

(*1. Department of Naval Architecture, Ocean and Marine Engineering, University of Strathclyde, G4 0LZ, Glasgow, UK;*

2. School of Energy and Power Engineering, Wuhan University of Technology, 430063, Wuhan, PR China;

3. Key Laboratory of Marine Power Engineering &Technology, Ministry of Communications, 430063, Wuhan, PR China;

**. Corresponding author*)

Abstract: The effects of seven matching parameters of a fuel injector and combustion chamber geometries on nitrogen oxide (NO_x), soot and specific fuel oil consumption (SFOC) were investigated by means of a parametric study. The study was carried out on four different engine loads, i.e. L25 (25%), L50 (50%), L75 (75%) and L100 (100%) loads. The injection-related parameters were found to have more prominent influences as opposed to the combustion chamber geometries. Then, a multi-objective genetic algorithm (MOGA) method was proposed in order to identify a set of optimal designs for the L100 load. The emissions and performance of these optimal designs were also examined and compared on the other three engine loads. Finally, an optimal design which meets the IMO (International Maritime Organization) Tier II NO_x emissions regulations (research shows it is impossible to meet Tier III NO_x emissions regulations solely on the basis of the optimisation of the combustion progress) and which has the best fuel economy was singled out.

Keywords: injector; combustion chamber; diesel engine; emission; fuel consumption

Nomenclature

2D	two dimensional	Simple	semi-implicit method for pressure linked equations
BTDC	before top dead centre	Sobol	quasi-random low-discrepancy sequences
CFD	computational fluid dynamics	SOI	start of injection
CO	carbon monoxide	SCR	selective catalytic reduction
CO_2	carbon dioxide	SR	swirl ratio
d003	connection length	TC	turbocharging
D2	a test cycle for NO_x emissions	TDC	top dead centre

[*] Corresponding author.

Email address: nao.hu.0128@gmail.com (N. Hu).

DoE	design of experiment	v001	the distance from the centre of toroidal surface to the piston top surface
ECAs	emission control areas	v002	clearance
EGR	exhaust gas recirculation	v003	crown centre height
GA	genetic algorithm		
h001	bowl radius	Functions and variables	
HC	hydrocarbons	x	n-dimensional parameter vector
HPCR	high-pressure common rail	f	function
IMO	international maritime organization	j	variable
KIVA	a Fortran-based CFD software	k	objective
L100	full engine load	N	maximum objective numbers
L25	25% engine load	$\vec{x}^*$	Pareto design
L50	50% engine load	$\vec{x}_j$	arbitrary design
L75	75% engine load		
MARPOL	the international convention for the prevention of pollution from ships	Units	
MOGA	multi-objective genetic algorithm	CA	crank angle
NLPQL	non-linear programming by quadratic Lagrangian	deg	degree
NO_x	nitrogen oxides	g/kWh	grams per kilowatt-hour
NPL	nozzle protrusion length	L	litre
Piso	pressure implicit split operator	kW	kilo Watt
r002	toroidal radius	mm	millimetre
SA	spray angle	r/min	rotates per minutes
SFOC	specific fuel oil consumption		

1 Introduction

Marine diesel engines play an indispensable role in shipping. Their extensive application as main propellers or generators mainly relies on their high reliability and fuel economy. However, intolerable pollutions caused by them are gaining increasing focuses worldwide. Compared to automotive diesel engines, marine diesel engines exhaust much lower CO, CO_2 and HC emissions, and conversely generate severely deteriorated NO_x emissions. As a result, the IMO expressly referred to the NO_x emissions in the revised Annex VI of MARPOL (Pueschel et al., 2013), as shown in Table 1. Tier II NO_x emission regulation came into force for engines mounted on a ship constructed on or after 1 January 2011. It stipulated the reduction of NO_x

up to 20% by comparing to Tier I regulations in the global area. The more stringent Tier III regulations were applied for engines installed on a ship constructed on or after 1 January 2016, operating in the ECAs. It requires a NO_x reduction of 80% from Tier I. Tier II regulations are still applied for ships operating outside of the ECAs.

Table 1 IMO NO_x emission regulations

Rated Speed n (r/min)	n<130	130≤n ≤2000	n>2000
Tier I (2000)/ g/(kWh)	17.0	$45 \cdot n^{-0.2}$	9.84
Tier II (2011)/ g/(kWh)	14.36	$44 \cdot n^{-0.23}$	7.66
Tier III (2000)/ g/(kWh) in ECAs	3.4	$9 \cdot n^{-0.2}$	1.97

In view of the challenge posed by stringent emission regulations, some existing technologies are applicable, for example, the EG), the SCR, the 2-stage TC system together with an extreme Miller cycle, the dual fuel engine or the nature gas operation (Christer, 2013; Steffe et al., 2013). However, some existing marine diesel engines installed on old ships can only meet the Tier I standard. Traditional mechanical fuel injection systems were widely mounted on these marine diesel engines. In order to improve their emission levels, a promising modification is to replace the mechanical injection systems with HPCR fuel injection systems. The flexible control over engine injection timing and injection quantity disregarding engine speed ensures that the HPCR systems achieve low emissions at all engine loads. Besides, high injection pressure (over 1000 bar) of the HPCR systems offers a finer fuel atomisation and a homogenous fuel-air mixing, which is beneficial to improving engine performance.

When a mechanical fuel injection system is replaced with a HPCR fuel injection system, the top priority is to decide the best match status between the fuel injection system and the combustion chamber. In this study, NO_x emissions, soot emissions and SFOC are selected as the three objectives to be minimised. The GA is frequently used in solving multi-objective problems. Many researchers have already applied this method for diesel engine optimisations. Researchers developed a KIVA code with a GA method in order to successfully study the matching of a variety of engine parameters, from small-bore high-speed direct injection engines to heavy-duty large-bore slow-speed diesel engines, even under different engine operation loads. This significant amount of engine optimisation work was conducted using the automatic grid generation tool and the effective optimisation algorithms (Kim et al., 2005; Genzale and Reitz, 2007; Genzale et al., 2008; Ge et al., 2009; Shi and Reitz, 2008a; Shi and Reitz, 2008b). Recently, Taghavifar et al. (2014) studied the effects of bowl movements and radius on the mixture formation in terms of the homogeneity factor, combustion initiation and emissions for a 1.8 L Ford diesel engine. They indicated that the mixture uniformity increased in line with the bowl displacement toward the cylinder wall, but at the same time also identified a rise in the combustion delay which substantially reduces the effective in-cylinder pressure. They also found that smaller bowl size contributes to a better squish and vortex formation in the chamber, although with lesser spray penetration and flame quenching. Park (2012) used a micro-genetic algorithm coupling with a KIVA code in order to optimise the combustion chamber geometry and the engine operating conditions for an engine fuelled with dimethyl ether. He found that the combustion and emission characteristics of the engine were significantly different from conventional diesel engines because of the properties of the fuel. Taghavifar et al. (2016) used a DoE method incorporated with a Sobol on order to scan through the various design points of a 1.8 L Ford diesel engine, with the purpose of identifying the reduction of NO_x and the enhancement of the spraying characteristics. They indicated that a low spray angle and a small bowl volume are beneficial to lowering emissions. Mobasheri and Peng (2012) investigated the influence of a re-entrant combustion chamber geometry on the mixture formation process, combustion process and engine performance of a high-speed direct injection diesel engine. They designed thirteen combustion chambers with different shapes by adjusting the piston goemetries, i.e. bowl depth, width, piston bottom surface and lip area. The results indicated that a small bowl diameter leads to high soot emissions, yet also implied that an optimal operating point was obtained with a slightly larger bowl diameter. Chen and Lv (2014) used an orthogonal design method in order to study the injection-related parameters match with three combustion chamber geometries for an 8.9 L Cummins diesel engine. Then, a NLPQL algorithm was adopted in order to optimise the detailed combustion chamber geometries.

Since most researchers invested their efforts and resources on the optimisation of automotive engines, little work has been conducted in relation to on marine medium-speed diesel engines. The effects of the injection-related parameters and combustion chamber parameters on emissions and fuel consumption were extensively studied, but no feasible solutions were identified on how to find a specific optimum which meets the emission regulations with the best fuel economy. Besides, optimal combustion chamber geometries may vary from engine type to engine type, due to the individual engine specifications and the match status of fuel injection systems with combustion chamber geometries.

In this paper, the HPCR fuel injection system match with the combustion chamber geometry of a marine medium-speed diesel engine was carefully investigated. The HPCR fuel injection system was designed and produced in order to replace the original mechanical fuel injection system mounted on the case marine medium-speed diesel engine (MAN 6L 16/24). It sought to meet a more stringent emission regulation and to also improve fuel economy. In the first place, a parametric study was carried out in order to get a general idea of how these design parameters affect the emissions and fuel economy. In the second place, MOGA algorithm was used in order to employ a set of optimal designs and operational parameters. Finally, an optimal design which meets the IMO Tier II emission regulations while maintaining a suitable fuel economy was selected. The complete optimisation scheme is shown in Fig. 1.

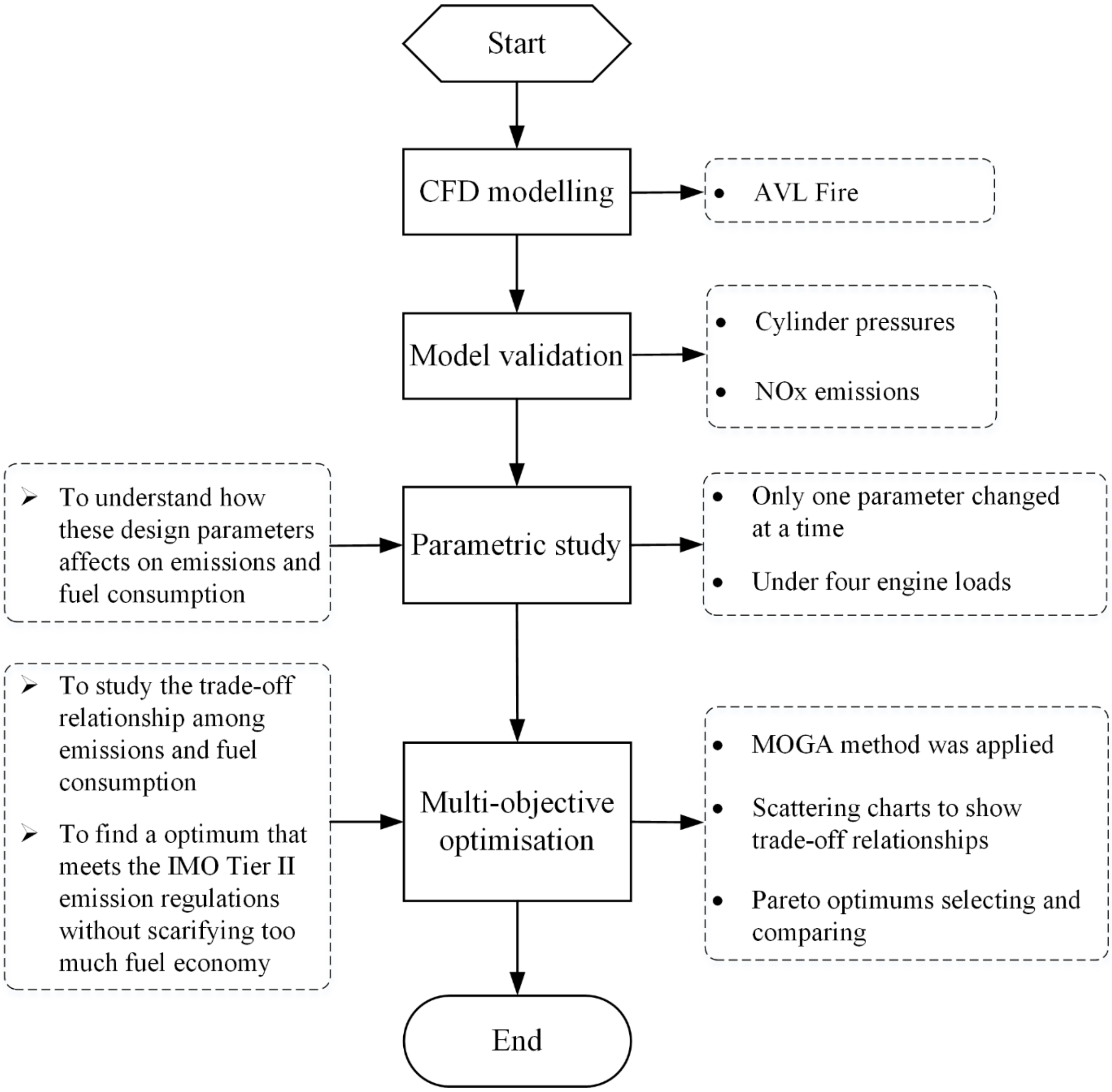

Fig. 1 Scheme of the optimisation process

2 Simulation model

Simulations were conducted by using a series of the AVL FIRE software. Firstly, the combustion chamber shape at TDC was drawn in Fire 2D Sketcher software according to the shape of the upper surface of the piston and the clearance distance between the piston surface and the cylinder head. The combustion chamber geometries were defined in this process. Secondly, the design combustion chamber geometries were loaded in the Fire ESE Diesel software in order to build a CFD model. In this instance, the k-zeta-f (Hanjalic et al. 2004; Popovac and Hanjalic, 2007) turbulent model for high Reynolds numbers is adopted in order to describe the flow field inside the combustion chamber. Simple/Piso algorithm (Versteeg and Malalasekera, 1995; Wanik and Schnel, 1989) is very suitable in order to solve the highly unsteady-state flow of the combustion problem. With regard to the fuel injection, the Dukowicz (Dukowicz, 1979) model is applied for handling the heat up and evaporation of the fuel oil droplets. Moreover, Wave (Reitz, 1987) break-up model and Walljet1 (Naber and Reitz, 1988; Cabrera and Gonzalez, 2003) wall interaction models are used respectively. The Eddy break-up model (Spalding, 1971; Magnussen and Hjertager, 1997) is introduced in the combustion calculation. An extended Zeldovich mechanism (Zeldovich et al., 1947) is adopted for the NO_x emission model while a Kinetic mechanism for the soot emission model (Apple et al., 2000; Balthasar and Frenklach, 2005). When the simulation model of the case engine is validated, a parametric study was conducted by using the CFD model built in Fire ESE Diesel software, where the design parameters need to be set as global variables for multi-objective study. Thirdly, the selected parameters were varied in the Fire DVI software, where the previously calculated CFD model was loaded and the response objectives were defined. Subsequently, the Fire Design Explorer software was invoked, where the design variables and their variation ranges, objectives, constraints and MOGA algorithm were specified. The combustion images were processed in the Fire Workflow Manager software.

3 Engine specifications and model verification

3.1 Engine specifications

The main geometric and performance specifications of the marine medium-speed diesel engine are presented in Table 2. The engine is an in-line, 6-cylinder and four-stroke diesel engine. Its rated speed and power are 1000 r/min and 540 kW, respectively. The spray orifice distribution of the original injector of the mechanical fuel injection system is 9*0.28 mm. The original fuel injector was replaced by an electronic fuel injector of 9*0.23 mm in the HPCR fuel injection system.

Table 2 Specifications of the engine and fuel injectors

Feature	Value
Engine name	MAN 6L16/24
Cylinder arrangement	In-line
Number of stroke	4
Bore(mm)	160
Stroke(mm)	240
Number of cylinders	6
Rated speed (r/min)	1000
Rated power (kW)	540
SFOC (g/(kW•h))	189
Compression ratio	15.2
Original injector	9*0.28 mm
Electronic fuel injector	9*0.23 mm

3.2 Model verification

The verification was executed at the rated engine speed and under four different engine loads, i.e. under the condition of 1000 r/m at the L25, L50, L75 and L100 loads. In order to improve the convergence at the beginning of the calculation, the initial calculation step is set to 0.2 deg

CA. Then, 1 deg CA is adopted at the compression stroke in order to accelerate calculation and save time as well. However, at the injection stage, the precision is emphasised by reducing the calculation step to the 0.2 deg CA again. In the expansion combustion stage, the 0.5 deg CA calculation step is adopted. The mesh of the original combustion shape at TDC is shown in Fig. 2.

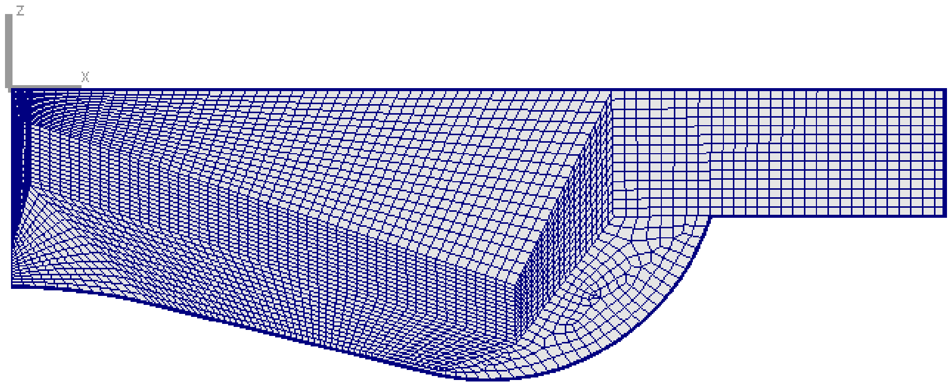

Fig. 2 Mesh at TDC

Fig. 3 shows comparisons of the cylinder pressures between the simulation data and the test data. The cylinder pressure was conveyed into charge signals by a KISTLER 6013C type cylinder pressure sensor and subsequently been conditioned to voltage signals by a charge amplifier before they were acquired by a high-speed data acquisition device. The voltage data was converted back into pressure data in a computer. From the figure, it can be seen that the simulation results match the experimental data well, especially in the combustion stage. In the stages of compression and expansion, the simulation data was a little bit larger than the test data, since the pressure losses induced by leakage were not considered in the simulation model. However, these losses do exist in the authentic diesel engine.

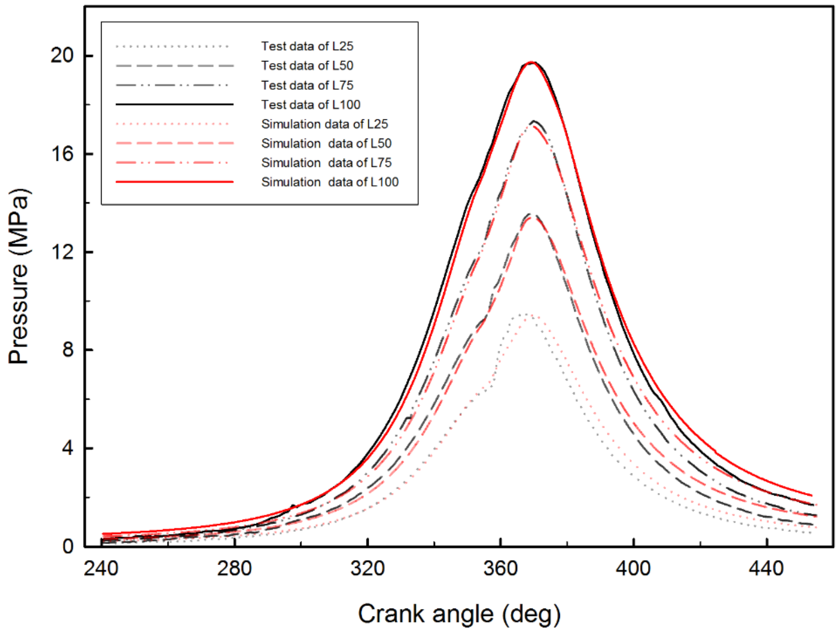

Fig. 3 Pressure comparisons of the experimental data and the simulation data

NO_x emissions are also examined at each load. The NO_x experimental data was provided by an engine producer, who performed the test under the standard D2 test cycle. It can be seen from Fig. 4 that the main trend of simulation results is corresponding with the test data. The maximum error between the simulation results and the test data is less than 6.5%, which occurred at the L100 load. The differences between the experimental and the simulation results might lie in the effects of test accuracy and test conditions. Sometimes the latter was also affected by the slight different in the composition of the fuels used in the test and simulation.

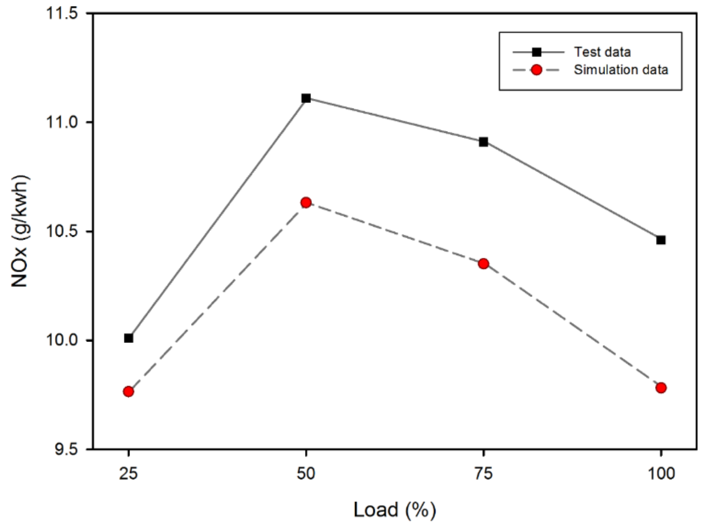

Fig. 4 NO_x emissions comparison of test data and simulation data

The aforementioned discussion indicates that the engine simulation model developed under FIRE can be used in order to simulate and predict the engine's performance when it is matching with a common rail injection system.

4 Parametric study

Injection-related parameters refer to the injection timing, the spray angle, the swirl ration and the nozzle protrusion length, whereas the combustion chamber geometry parameters refer to the bowl diameter, the toroidal radius and the centre crown height. Fig. 5 demonstrates the overall shape of the combustion chamber; the bowl diameter is twice the size of the h001. The toroidal radius is represented by the r002 and the centre crown height is represented by the v003. Other geometries such as v001, v002 and d003 are adjusted automatically in the software in order to maintain the same compression ratio.

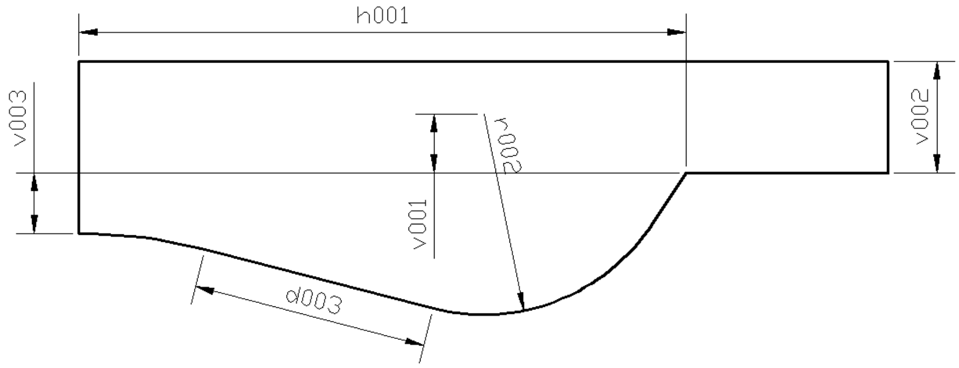

Fig. 5 Sketch of the combustion chamber geometries

The variation ranges of the injection-related parameters and the combustion chamber geometries used for the parametric study and for the match optimisation are listed in Table 3. The simulation steps are only useful in the parametric study. The baseline design in this instance refers to the original engine with its mechanical fuel injection system being replaced by a HPCR fuel injection system. The fuel injector orifice is also changed from 9*0.28 mm to 9* 0.23 mm, whereas other parameters remained the same as in the case of the original engine. The NO_x emissions, soot emissions and SFOC are the three objectives to be minimised.

Table 3 Variation ranges of the parameters used for the parametric study and for the match optimisation

Items	Parameters	Baseline	Lower Bound	Upper Bound	Step
Injection-related parameters	SOI, deg BTDC	10	20	0	5
	SR, -	1	0.5	2.5	0.5
	SA, deg	143	131	155	6
	NPL, mm	2.5	1.0	4.0	0.75
Combustion chamber geometries	r002, mm	20	18	22	1
	v003, mm	6	5	9	1
	2*h001, mm	120	108	132	6

The variation ranges of the three combustion chamber geometries were demonstrated in Fig. 6, where the black line represents the shape of the original and baseline combustion chamber, whereas the green and the pink lines indicate the lower bound and the upper bound of the combustion chamber geometries respectively.

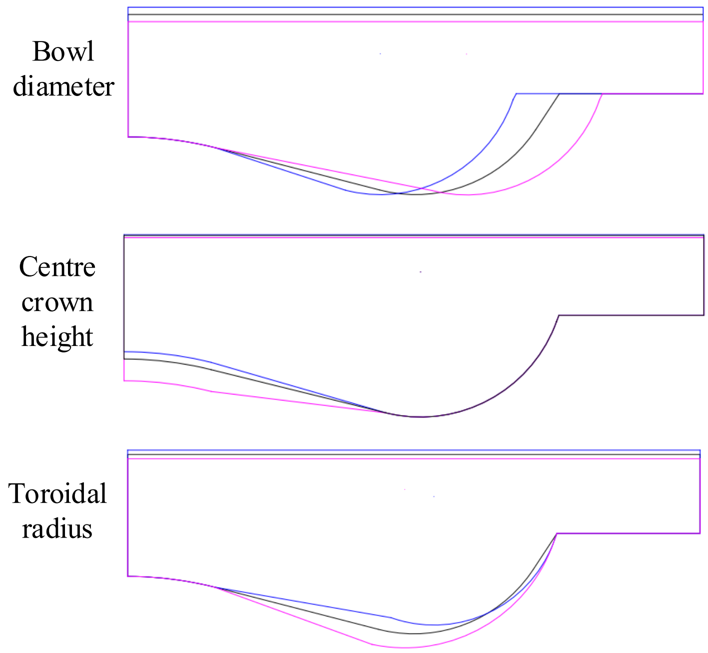

Fig. 6 Variation ranges of the combustion chamber geometries

The results of the parametric study are shown in Fig. 7 and Fig. 8. From Fig. 7, it can be seen that the injection timing has the most influence on the objectives. With the increase in injection timing, a monotonic increasing trend of the NO_x emissions is observed. On the contrary, an opposite decreasing trend is observed in the SFOC. The NO_x emissions at 20 degrees BTDC are approximately three times higher than that at the TDC. The SFOC decreases by nearly 20% from the TDC to 20 degrees BTDC. When the injection occurs at the 20 degrees BTDC, sufficient time for fuel vaporisation and fuel-air mixing results in fierce combustion and high temperatures. A high temperature facilitates the generation of NO_x emissions. Fortunately, sufficient mixing is beneficial for a complete combustion, which is good for achieving a high fuel economy and a low SFOC. Conversely, soot emissions, decrease in line with the increasing in injection timing, due to the fact that a complete combustion helps reduce soot formation.

Inversed impacts at the level of the objectives can be seen with the increase in the spray angle and nozzle protrusion length. In detail, NO_x increases in line with the increase in the spray angle, while soot and SFOC drop at the same time. Larger influences on the soot formation are reported at low engine loads (L25 and L50 loads). When spraying occurred at 131 degrees, most of the fuel was ejected into the bowl area and adhered to the surface of the piston. It was unfavourable for the NO_x formation especially when the piston was going downward, the volume of the combustion chamber expanded and the temperature dropped. Most of the fuel did not burn completely and was exhausted in the form of soot emissions, which explains the higher soot emissions and the deteriorated fuel economy as opposed to the results obtained at any other angles. This kind of phenomenon alleviates greatly with the increase in the spray angle, especially when the injection angle increases to 155 degrees. The fuel was split into the bowl area and the clearance area. A reduced fuel density and enhanced fuel vaporisation contribute to a more homogeneous fuel distribution. Thus, attractive low soot emissions and SFOC were achieved. However, the NO_x emissions were sustained at a high level because of the high temperature under such circumstances.

As for the influences of the nozzle protrusion length on the objectives, the NO_x emissions decrease along with the increase in the nozzle protrusion length. The lower the load is, the faster the drop rate. The SFOC shows approximately an opposite trend to the NO_x emissions. With regard to the soot emissions, these rise quickly when the nozzle protrusion length becomes larger than 2.5 mm on L25 and L50 loads, while keeps nearly the same on L75 and L100 loads. As the nozzle protrusion length increases, the injection spray targets the bottom area of the bowl. From this point, the effect of increasing the nozzle protrusion length is the same as decreasing the injection angle. More specifically, the distance between the injector and the piston surface exposed to the injection direction becomes shorter, which means that more fuel hits and adheres to the surface of the piston bowl. The fuel on the piston surface is difficult to be burned completely and is then exhausted as soot emissions. Therefore, increasing the nozzle protrusion length increases the soot emissions and the SFOC, but reduces the NO_x emissions slightly, since the low temperature suppresses the NO_x formation in the combustion process.

The effects of swirl ratio on the emissions and on the fuel consumption are also not negligible. The NO_x emissions increase in line with the increase in the swirl ratio at high loads (L75 and L100 loads). However, the NO_x emissions remain nearly the same at low loads. For soot emissions, an increasing trend is observed as the swirl ratio increases. The SFOC reports an increasing trend at low loads. However, the SFOC is not affected much by the swirl ratio at high loads. In theory, a strong swirl reduces the ability of the fuel penetration, however, when the swirl is too strong, this can be unfavourable for ignition, which in turn delays the combustion process. Thus, some fuel is incompletely burned off before being exhausted, which causes high soot emissions and SFOC. However, a moderate swirl ratio promotes the fuel-air mixing, which is better for reducing soot emissions and SFOC.

262
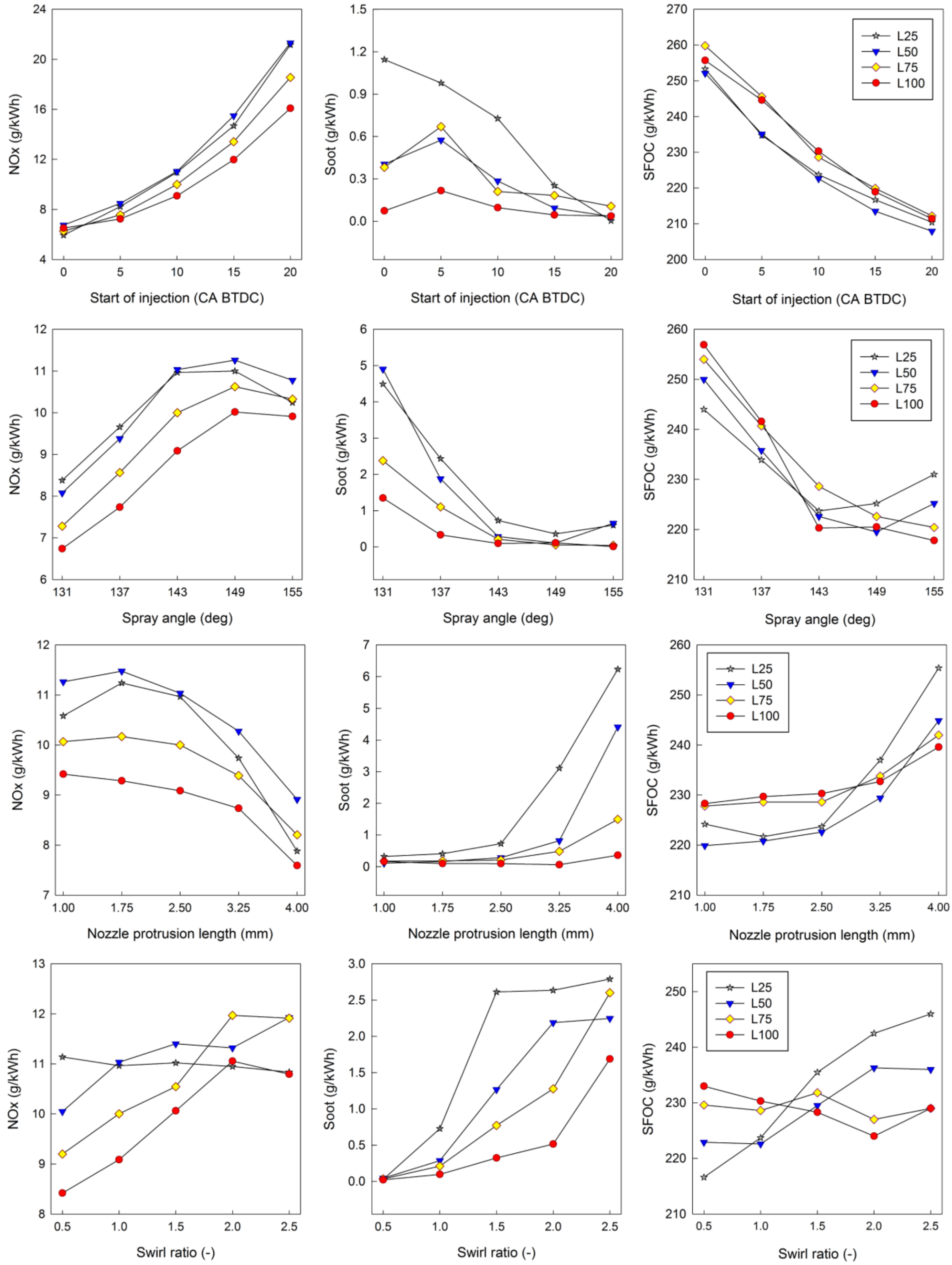

263 Fig. 7 Influences of the injection-related parameters on the objectives

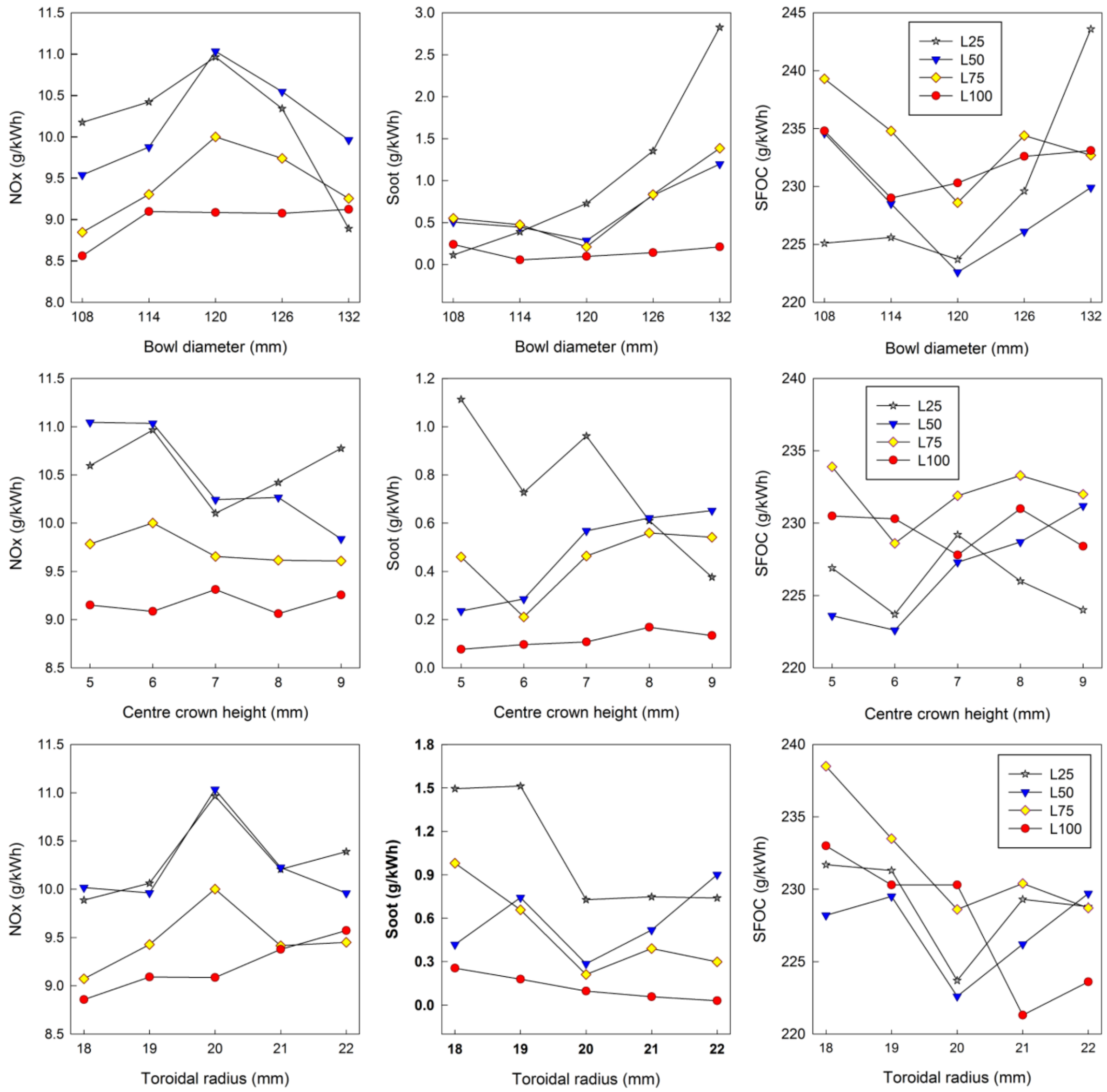

Fig. 8 Influences of the combustion chamber geometries on the objectives

From Fig. 8, in general, it may be inferred that the bowl diameter and the toroidal radius have a larger impact on the objectives as opposed to the centre crown height. The bowl diameter mainly affects the objectives under low loads, whereas the NO_x emissions increase in line with the increase in the bowl diameter and reach a peak when the bowl diameter is 120mm before they gradually decline. An opposite trend is witnessed for the SFOC. With regard to soot emissions, they were little affected by the bowl diameter at the L100 load. Soot emissions decrease in line with the increase in the bowl diameter and meets a valley when bowl diameter is 120 mm, then increase to nearly three times of their original value. A small bowl diameter means that more fuel hits on the surface of the piston and adheres hereto, thus, some fuel is not able to evaporate and atomise in time, which leads to an incomplete combustion. This explains why soot emissions and SFOC were high when the bowl diameter was small. At the same time, the low maximum temperature of the incomplete combustion circumstance is unfavourable for the formation of NO_x emissions. When the bowl diameter increases, the incomplete combustion alleviates, the temperature rises, soot emissions and SFOC decrease and NO_x emissions increase at the same time. This trend reverses when the bowl diameter is larger than 120mm. A large bowl diameter implies a longer distance between the fuel injector and the surface of the piston bowl area. Most of the fuel is injected targeting solely the bowl area of the piston in order to form a high-density mixture, which is not favourable for a complete combustion. Meanwhile, it encourages soot formation and leads to high levels of the SFOC. At the same time, a slightly low maximum temperature is achieved in order to generate a reduced number of NO_x emissions, by making a comparison with the moderate bowl diameter case.

With the increase in the toroidal radius, the NO_x emissions increase slowly, whereas the opposite may be observed in the case of the soot emissions and SFOC decrease slowly. No obvious trends were seen for the influences of the centre crown height on the objectives, and thus, the centre crown height has a limited impact on the objectives.

From the discussion above, one has to notice that the injection related parameters have a more significant influence on emissions and fuel consumption as opposed to the combustion chamber geometries. It explains why marine medium-speed diesel engines rely on the injection spray in order to improve their fuel-air mixing. This type of features differentiates marine medium-speed diesel engines from the small size engines, in which re-entrant combustion chambers are frequently adopted in order to promote fuel-air mixing during high-speed operations (Wickman et al., 2001 and Taghavifar et al., 2014).

The parametric study indicates the impacts of the injection-related parameters and the combustion chamber geometries on emissions and fuel consumption independently. It is easy to find the best value for each parameter under such conditions, however, whether these best parameters would form a good design or not still remains uncertain. Under these circumstances, a further study was carried out using a global optimisation method referred to as MOGA in order to seek an optimal design, which meets the IMO Tier II emission regulations and which has the best fuel economy. The optimisation study was conducted only at L100 load due to the time consuming CFD calculation process.

5 Optimisation with the MOGA method

5.1 Optimisation method

The GA is based on the idea of the natural selection which obeys the law of 'survival of the fittest'. It can continually improve the average fitness level of a population by means of inheritance, mutation, selection and crossover. Eventually, the optimisation process leads to an optimal design (Senecal et al. 2002). MOGA is the modification version of the GA in order to find a set of multiple non-dominated solutions in a single run (Konak et al., 2006).

The Pareto optimum is often adopted in the case of a multi-objective optimisation process, as shown in Fig. 9. Cases A-D can be considered as Pareto optimal cases due to the fact that none of them outperformed by the other cases. These cases can be grouped together in order to form a Pareto front (Shi and Reitz, 2008). The Pareto optimality can be defined as: For all designs and the corresponding N objectives $f_k(\vec{x})$, where, K= 1, 2, …, N, the Pareto design $\vec{x}$ is defined as follows: for an arbitrary design j, there is at least one objective, k, which meets the condition $f_k(\vec{x}_j) \le f_k(\vec{x})$. MOGA's mission is to find the Pareto front while maintaining diversity in the results (Salvador et al. 2014; Ge et al., 2009).

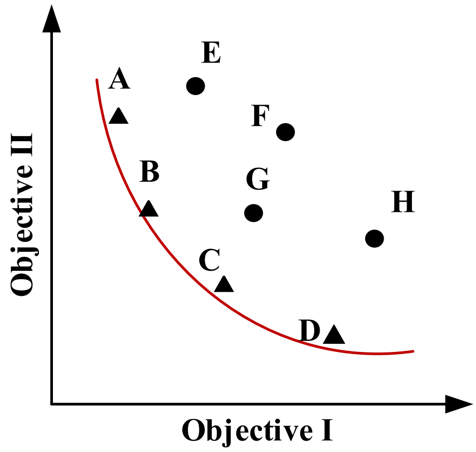

Fig. 9 Definition of the Pareto optimum

5.2 Optimisation settings

The variation ranges of the parameters are the same with the ones used in the parametric study, as shown in Table 3. The optimisation settings of the MOGA method are listed in Table 4. The distribution for the crossover and for the mutation probabilities are both set as the default value 10. The generation number of 10 and the population size of 20 are adopted here. This means that a total of 200 cases are generated and calculated by means of the MOGA method. Usually, the crossover probability and mutation probability are set to 0.7 and 0.1, respectively.

Table 4 Optimisation setting of the MOGA method

Property	Value
Distribution for crossover probability	10.0

Distribution for Mutation Probability	10.0
Number of Generations	10
Population size	20
Crossover Probability	0.7
Mutation Probability	0.1

5.3 Results discussion

Fig. 10 and Fig. 11 show the optimisation results of the L100 load by using the MOGA method. The black dot lines indicate the Tier II emission limit for the case engine. The black square point A represents the original engine, and the black solid circle B represents the baseline engine. The blue hollow triangles marked C, D and E are the selected Pareto optimal designs. From the figure, it can also be noticed that even the best NO_x design point still cannot meet the IMO Tier III regulation, which requires the NO_x emissions to be lower than 2.26 g/kWh for the case engine.

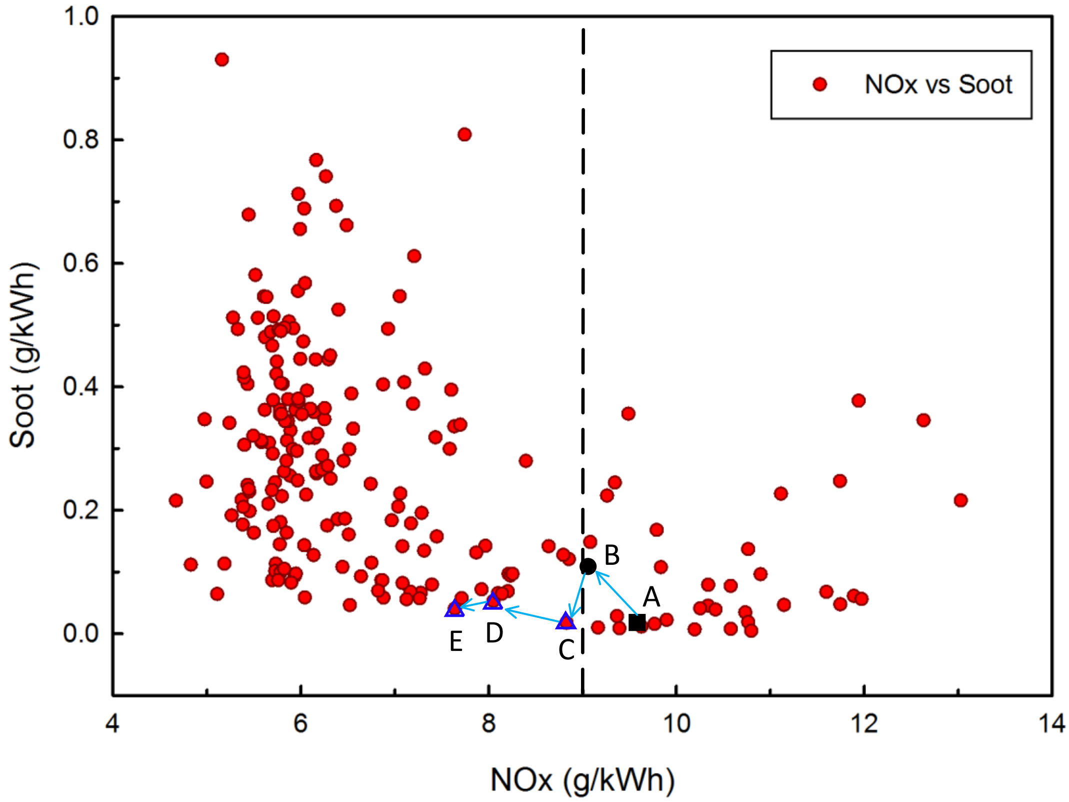

348

349 Fig. 10 NO_x emissions vs. the soot emissions of the L100 load

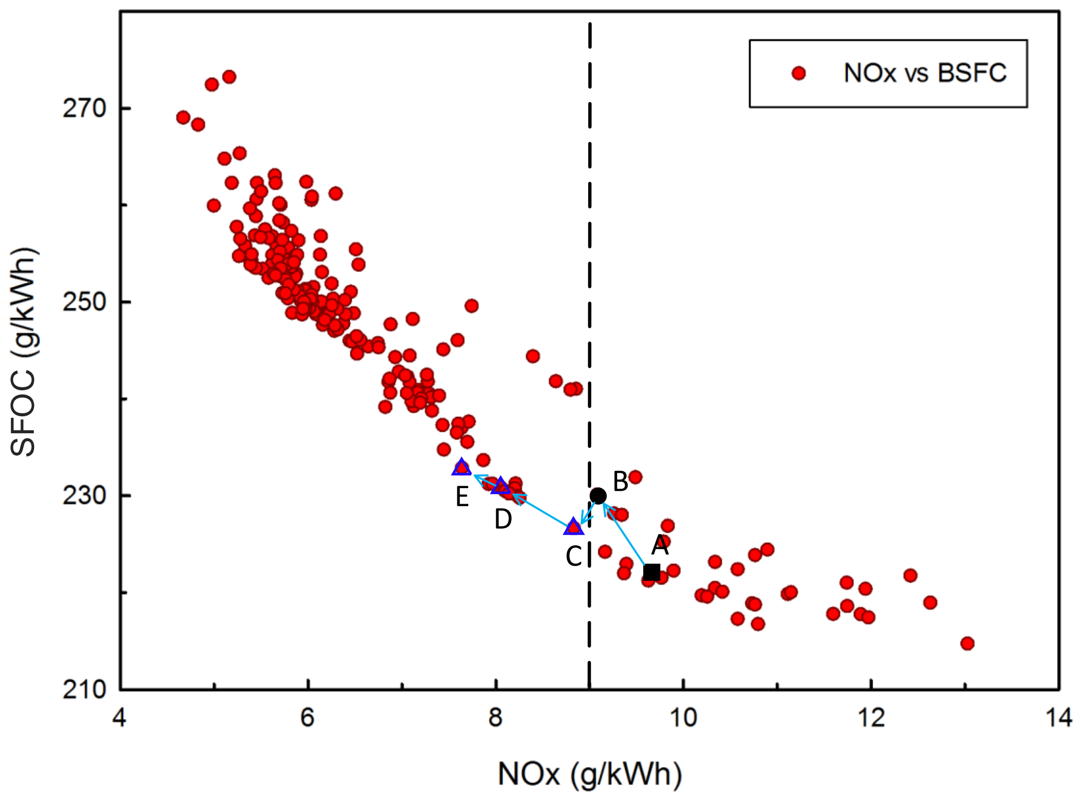

Fig. 11 NO_x emission vs. the SFOC of the L100 load

Table 5 gives objectives' values of the original engine, baseline and selected Pareto optimal designs. The corresponding design parameters are shown in Table 6. Compared to the original engine, it can be seen that the baseline design reduced nearly 7% of the NO_x emissions, but it still fails to comply with the IMO Tier II regulations. Besides, it has a penalty of a 5 time' increase of soot emissions and a 2.7% increase of SFOC than the original engine. The Pareto optimums C, D and E meet the requirement of the IMO Tier II regulations on the L100 load in addition to also having low soot emissions as well. Comparisons of their performance under the other three engine loads (L75, L50 and L25 loads) were also carried out for inspection. The results are shown in Fig. 12, Fig. 13 and Fig. 14.

Table 5 Comparisons of the optimisation objectives of the L100 load

L100 load	NO_x (g/kWh)	Soot (g/kWh)	SFOC (g/kWh)
Original type A	9.78	0.016	224
Baseline B	9.09	0.096	230
Optimum C	8.83	0.017	227
Optimum D	8.05	0.053	231
Optimum E	7.64	0.041	233

Table 6 Comparisons of the deign parameters

Design	SOI (CA) BTDC	Swirl ratio	Spray angle (deg)	Nozzle protrusion length (mm)	Bowl diameter (mm)	Height of centre crown (mm)	Toroidal radius (mm)
Original type A &Baseline B	10	1	143	2.5	120	6	40
Optimum C	12	0.54	151	2.4	116.64	6.73	40.80
Optimum D	9	0.98	151	3.4	118.41	6.24	40.58
Optimum E	9	0.56	151	3.4	118.28	6.66	40.58

Fig. 12 shows that the optimums D and E perform well in NO_x emissions which meet the IMO Tier II emission regulations. Conversely, the optimum C fails, despite having the lowest soot emissions and SFOC, as shown in Fig. 13 and Fig. 14. Optimum D and optimum E show negligible differences in soot emissions and SFOC at the L100 load, but optimum D performs poorly in other engine loads, i.e., soot and SFOC increase greatly with the decrease in the engine load. On the contrary, optimum E behaves steadily and thus constitutes to be the best choice.

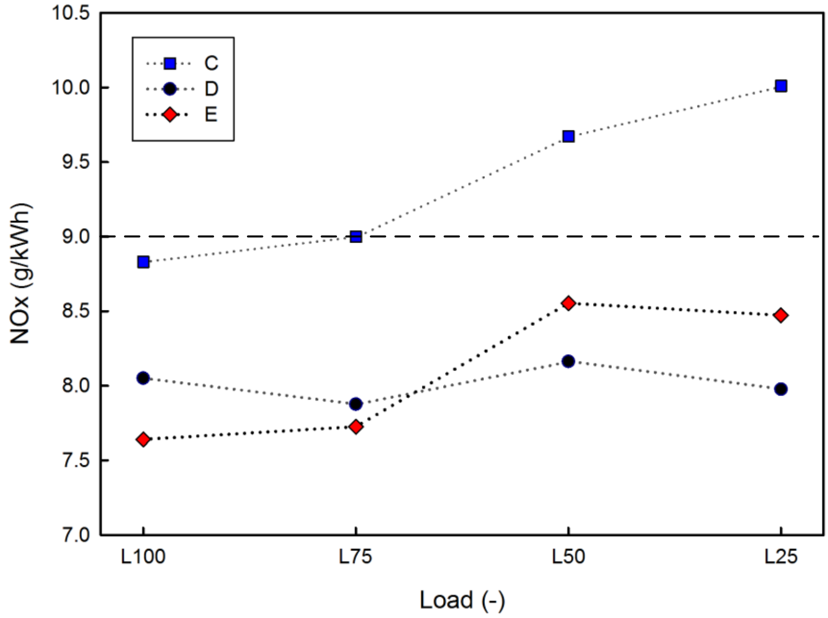

Fig. 12 NO_x comparisons of the selected Pareto optimums in all four engine loads

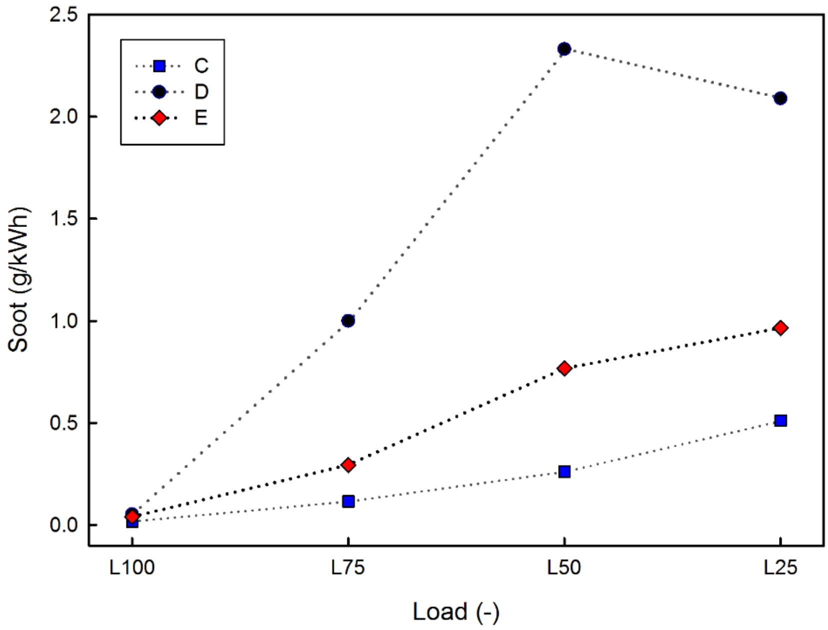

Fig. 13 Soot comparisons of the selected Pareto optimums in all four engine loads

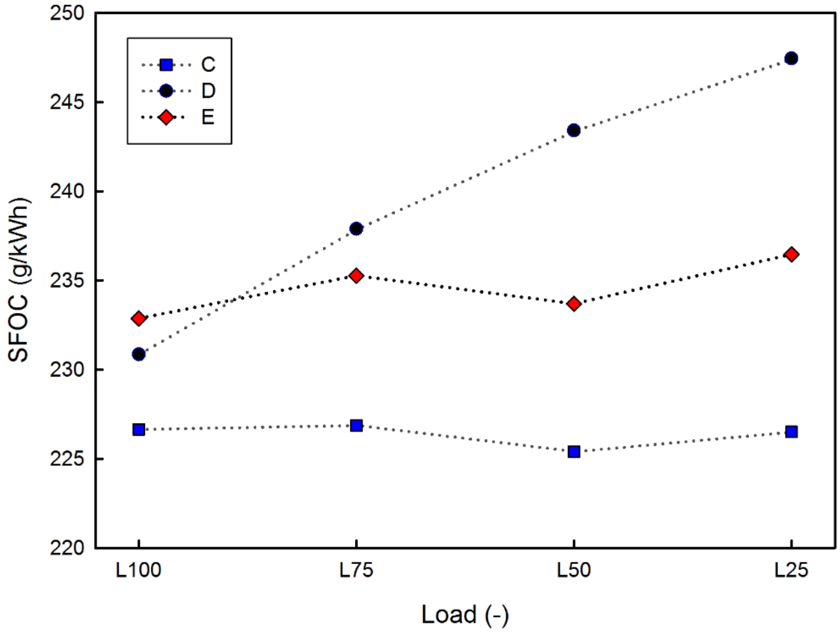

Fig. 14 SFOC comparisons of the selected Pareto optimums in all four engine loads

Fig. 15 gives the detailed information about the combustion progress comparisons. It can be clearly seen from Fig. 15 (c) that the rate of heat release of the original engine is much higher than that of the baseline design and of the optimum E. It leads to a higher combustion temperature which is favourable for the NO_x formation, and thus the NO_x emission level is higher than the baseline and the optimum E design, as shown in Fig. 15 (a) and (d). In the case of optimum E, the rate of heat release lasts longer, which means that the highest temperature in the combustion chamber is lower than the baseline design. Lower temperature suppresses the formation of NO_x, and as a result, the NO_x emission level is the lowest among the three designs. The soot formation of the baseline design is much higher than other designs, answers can be obtained the form Fig. 16, which indicates that at 60 degrees after the TDC, there is still a large quantity of fuel gathering around the piston bowl area and the top surface of the combustion chamber. It led to an incomplete combustion, and also to the high soot formation and high SFOC. On the contrary, optimum E gained a more homogeneous fuel distribution, which helps reduce the soot formation.

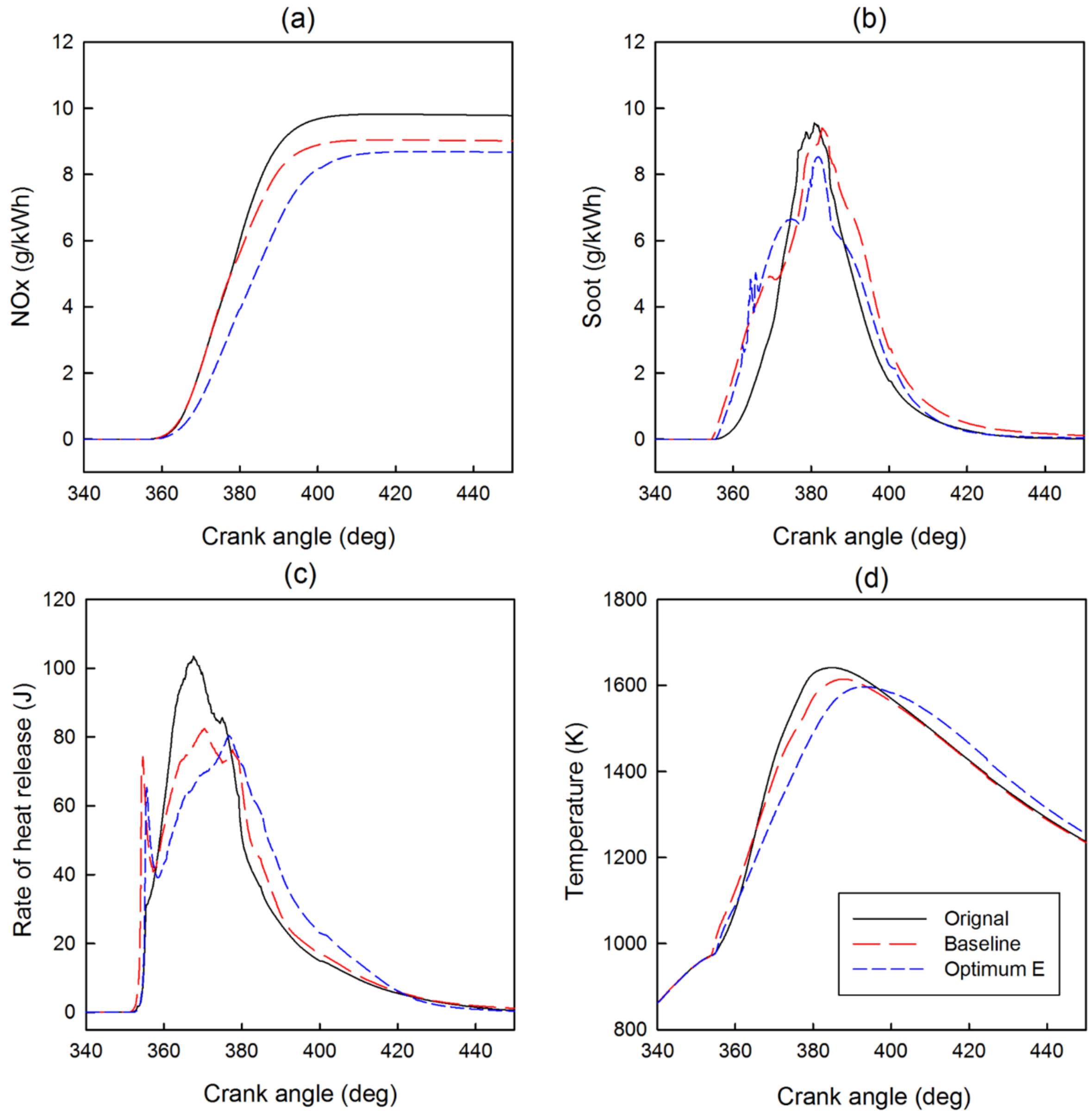

Fig. 15 Detailed comparisons of the original, baseline and optimum E designs

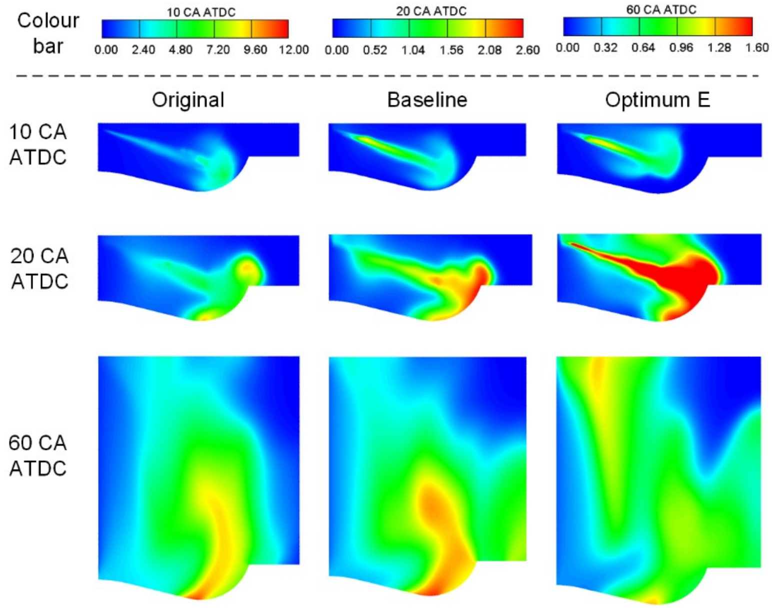

Fig. 16 CFD comparisons of the original, baseline and optimum E designs

6 Conclusions

The parametric study was conducted in order to investigate the effects of four injection-related parameters and three combustion chamber geometries on NO_x emissions, soot emissions and SFOC respectively. Then, the MOGA method was introduced in order to find an optimal design which meets the IMO Tier II emission regulations and meanwhile has the best fuel economy. In this instance, the performance of three selected Pareto designs C, D and E of the L100 load were compared and examined under the other L75, L50 and L25 engine loads. The optimum E outperforms other selected Pareto designs. Finally, the original, baseline and optimum E designs were extensively compared in details in order to dig the reasons why optimum E performs better. The main conclusions are listed as follows:

(1) Injection-related parameters have more significant impacts on the objectives as opposed to the combustion chamber geometries within the research scope.

(2) Injection timing has the greatest impact on the objectives, especially on the NO_x emissions.

(3) Low NO_x emissions prefer the late injection and the low swirl.

(4) The MOGA method is an effective way to solve the problem of the fuel injector match with the combustion chamber by providing a set of Pareto designs.
(5) A routine is presented for finding a Pareto optimum which meets the IMO Tier II emission regulations and also maintains the best fuel economy.

Acknowledgment

Authors are grateful to the Department of Naval Architecture and Marine Engineering of University of Strathclyde for the calculation support on the project. We also appreciate the Wuhan University of Technology for providing experimental facilities and test data.

Funding: This work was supported by the project of 'An Investigation into the Characteristics of High-pressure Common Rail Injection System' from Lloyds Register of Shipping of UK and the project of 'Engineering Development of a Medium-Speed Dual Fuel Engine (Ministry of Industry and Information Technology NO. (2013) 412, 2)' from China.

Reference

Apple, J., Bockhorn, H., Frenklach, M., 2000. Kinetic modelling of soot formation with detailed chemistry and physics: laminar premixed flames of C2 hydrocarbons. Combustion and Flame 121 (2000), 122-136.

Balthasar, M., Frenklach, M., 2005. Detailed kinetic modelling of soot aggregate formation in laminar premixed flames. Combustion and Flame 140(2005), 130-145.

Cabrera, E., Gonzalez, J.E., 2003. Heat flux correlation for spray cooling in the nucleate boiling regime, Exp. Heat Transfer 16(2003), 19-44.

Chen, Y., Lv, L., 2014. The multi-objective optimization of combustion chamber of DI diesel engine by NLPQL algorithm. Applied Thermal Engineering 73(2014), 1332-1339.

Christer, W., 2013, Tier III technology development and its influence on ship installation and operation, CIMAC Congress 2013, Shanghai, Paper no: 159.

Dukowicz, J.K., 1979. Quasi-steady droplet change in the presence of convection, Los Alamos Scientific Laboratory, LA7997-MS.

Ge, H.W., Shi, Y., Reitz, R.D., 2009. Optimization of a HSDI diesel engine for passenger cars using a multi-objective genetic algorithm and multi-dimensional modelling. SAE Int. J. Engines, 2009-01-0715.

Genzale, C.L., Reitz, R.D., 2007. A computational investigation into the effects of spray targeting, bowl geometry and swirl ratio for low-temperature combustion in a heavy-duty diesel engine. SAE Technical Paper Series, 2007-01-0119.

Genzale, C.L., Reitz, R.D., Musculus, M.P.B., 2008. Effects of piston bowl geometry on mixture development and late-injection low-temperature combustion in a heavy-duty diesel engine. SAE Int. J. Engines 1(1), 2008-01-1330.

Hanjalic, K., Popovac, M., Hadziabdic, M., 2004. A robust near-wall elliptic relaxation eddy-viscosity turbulence model for CFD. International Journal of Heat and Fluid Flow 25(2004), 1047-1051.

Kim, M., Liechty M.P., Reitz, R.D., 2005. Application of micro-genetic algorithms for the optimization of injection strategies in a heavy-duty diesel engine. SAE Technical Paper Series, 2005-01-0219.

Konak, A. Coit, D.W., Smith, A.E., 2006. Multi-objective optimization using genetic algorithms: A tutorial. Reliability Engineering and System Safety 91 (2006), 992-1007.

Magnussen, B.F., Hjertager, B.H., 1997. On mathematical modelling of turbulent combustion with special emphasis on soot formation and combustion. Symposium (International) on Combustion 16(1), 719-729.

Mobasheri, R., Peng, Z.J., 2012. Analysis of the effect of re-entrant combustion chamber geometry on combustion process and emission formation in a HSDI diesel engine. SAE International, 2012-01-0144.

Naber, J.D., Reitz, R.D., 1988. Modelling engine spray/wall impingement. SAE, 880107.

Park, S., 2012. Optimization of combustion chamber geometry and engine operating conditions for compression ignition engines fueled with dimethyl ether. Fuel 97, 61-71.

Popovac, M., Hanjalic, K., 2007. Compound wall treatment for RANS computation of complex turbulent flows and heat transfer. Flow Turbulence and Combustion 78(2007), 177-202.

Pueschel, M., Buchholz, B., Fink, C., Rickert, C., Ruschmeyer, K, 2013. Combination of post-injection and cooled EGR at a medium-speed diesel engine to comply with IMO Tier III emission limits. CIMAC Congress 2013, Shanghai.

Reitz, R.D., 1987. Modelling atomization processes in high-pressure vaporizing sprays, Atomization and Spray Technology 3(1987), 309-337.

Salvador, F.J., Plazas, A.H., Gimeno, J., Carreres, M., 2014. Complete modelling of a piezo actuator last-generation injector for diesel injection systems. International J of Engine Research 15(1), 3-19.

Senecal, P.k., Pomraning, E., Richards, K.J., 2002. Muti-mode genetic algorithm optimization of combustion chamber geometry for low emissions. SAE 2002 World Congress, 2002-01-0958.

Shi, Y., Reitz, R.D., 2008a. Assessment of optimization methodologies to study the effects of bowl geometry, spray targeting and swirl ratio for a heavy-duty diesel engine operated at high-load. SAE Int. J. Engines, 2008-01-0949.

Shi, Y., Reitz, R.D., 2008b. Optimization study of the effects of bowl geometry, spray targeting, and swirl ratio for a heavy-duty diesel engine operated at low and high load. Int. J. Engine Res. 9, 325-346.

Spalding, D.B., 1971. Mixing and chemical reaction in steady confined turbulent flames. Symposium (International) on Combustion 13(1), 649-657.

Steffe, P., Liepert, K. Losher, R., Bader I., 2013. High performance solutions for IMO TIER III-system integration of engine and after treatment technologies as element of success. CIMAC Congress 2013, shanghai, paper no: 212.

Taghavifar, H., Jafarmadar. S., Taghavifar, H., Navid, A., 2016. Application of DoE evaluation to introduce the optimum injection strategy-chamber geometry of diesel engine using surrogate epsilon. Applied Thermal Engineering 106, 56–66.

Taghavifar H, Khalilarya S, Jafarmadar S., 2014. Engine structure modifications effect on the flow behavior, combustion, and performance characteristics of DI diesel engine. Energy Conversion and Management 8, 20-32.

Versteeg, H.K., Malalasekera, W., 1995. An Introduction to computational fluid dynamics the finite volume method. Longman Scientific & Technical. ISBN 978-0131274983.

Wanik, A., Schnel, U., 1989. Some remarks on the PISO and SIMPLE algorithms for steady turbulent flow problems. Computers & Fluids 17(4), 555-570.

Wickman D.D., Senecal P.K., Reitz R.D. Diesel Engine Combustion Chamber Geometry Optimization Using Genetic Algorithms and Multi-Dimensional Spray and Combustion Modeling. SAE Technical Paper Series, 2001-01-0547.

Zeldovich, Y.A., Frank-Kamenetskii, D., Sadovnikov, P., 1947. The oxidation of nitrogen in combustion and explosions. Publishing House of the Academy of Sciences of USSR.